

Bayesian Parametric Portfolio Policies

Miguel C. Herculano*

This Version: February 2026

Abstract

Parametric Portfolio Policies (PPP) estimate optimal portfolio weights directly as functions of observable signals by maximizing expected utility, bypassing the need to model asset returns and covariances. However, PPP ignores policy risk. We show that this is consequential, leading to an overstatement of expected utility and an understatement of portfolio risk. We develop Bayesian Parametric Portfolio Policies (BPPP), which place a prior on policy coefficients thereby correcting the decision rule. We derive a general result showing that the utility gap between PPP and BPPP is strictly positive and proportional to posterior parameter uncertainty and signal magnitude. Under a mean–variance approximation, this correction appears as an additional estimation-risk term in portfolio variance, implying that PPP overexposes when signals are strongest and when risk aversion is high. Empirically, in a high-dimensional setting with 242 signals and six factors over 1973–2023, BPPP delivers higher Sharpe ratios, substantially lower turnover, larger investor welfare, and lower tail risk, with advantages that increase monotonically in risk aversion and are strongest during crisis episodes.

Keywords: Portfolio choice; Bayesian decision theory; factor timing; estimation risk.

JEL Codes: G11, C11, C52.

arXiv:2602.21173v1 [q-fin.PM] 24 Feb 2026

*Adam Smith Business School, University of Glasgow. E: miguel.herculano@glasgow.ac.uk. W: mherculano.github.io

1 Introduction

A central problem in asset pricing is to translate predictive information into portfolio decisions in a way that is both economically meaningful and empirically robust. Decades of research document that expected returns vary predictably with firm characteristics and macroeconomic signals (Chen and Zimmermann, 2022; Gu et al., 2020; Haddad et al., 2020), yet exploiting such predictability in real time remains challenging. Classic mean-variance approaches require modelling the joint conditional distribution of returns, a task that quickly becomes infeasible in high-dimensional settings and is known to produce unstable weights in finite samples (DeMiguel et al., 2009; Green et al., 2017). Parametric Portfolio Policies (PPP), introduced by Brandt et al. (2009), offer an appealing solution. Rather than modelling returns, PPP parameterise portfolio weights directly as functions of observable predictors and estimate policy parameters by maximising average realised utility.

PPP rests on a strong implicit assumption that motivates this paper. Once the policy parameter θ is estimated, the investor behaves as if $\hat{\theta}$ were the true data-generating policy, ignoring the uncertainty surrounding such estimate. We show that this treatment of policy uncertainty is consequential, leading to a systematic overstatement of investor welfare and understatement of portfolio risk. Moreover, these effects are largest when risk aversion is high or signals are strong, exactly when PPP takes its most aggressive positions. We adopt a Bayesian perspective and treat the policy parameter θ as a random variable. Bayesian Parametric Portfolio Policies (BPPP) places a prior on θ and integrates expected utility over the resulting posterior, internalizing policy risk and producing more stable portfolio allocations. Crucially, this stability is not imposed through an *ad hoc* penalty or constraint. It arises directly from rational investor behaviour under concave utility and uncertain parameters. In a mean-variance approximation, the BPPP correction adds an estimation-risk term to the variance of portfolio returns, shrinking tilts proportionally.

Several aspects of the framework are worth emphasising. First, BPPP nests PPP as the

special case of a flat (uninformative) prior, in which the posterior collapses to a point mass at $\hat{\theta}$. Second, the framework requires no distributional assumptions on returns beyond those already embedded in the utility function. Third, from an empirical viewpoint BPPP accommodates an additional source of information for portfolio construction, via the prior which allows for the inclusion of investor's *ex-ante* beliefs about how aggressively the policy should respond to signals.

We evaluate BPPP by using six Fama–French factor portfolios, 242 predictive signals (212 anomaly-based predictors from [Chen and Zimmermann \(2022\)](#) and 30 factor-timing signals following [Haddad et al. \(2020\)](#)), and an expanding-window out-of-sample exercise from 1973M8 to 2023M12. This high-dimensional environment is precisely the setting where parameter uncertainty is large and the overstatement predicted is most severe. BPPP achieves a gross out-of-sample Sharpe ratio of 1.32, versus 1.05 for PPP and 0.74 for the market benchmark. Under CRRA utility with moderate risk aversion ($\gamma = 5$), BPPP delivers a certainty-equivalent advantage of 536 basis points per annum relative to the market benchmark, compared with 353 basis points for PPP. The gap widens with risk aversion, at $\gamma = 10$ the difference is about 255 basis points, consistent with the prediction that the overexposure correction matters most for risk averse investors. Turnover falls materially relative to PPP, and at 50 basis points of transaction costs BPPP retains a net Sharpe near 0.99 versus 0.60 for PPP. The BPPP advantage holds in four of the five complete decades of the sample and in both major crisis episodes (the Great Financial Crisis and Covid). The Bayesian approach also yields portfolios with lower tail risk.

Our paper contributes to several strands of the literature. The classical Bayesian portfolio choice literature ([Kandel and Stambaugh, 1996](#); [Pástor and Stambaugh, 2000](#); [Barberis, 2000](#)) shows that parameter uncertainty leads to more conservative allocations when modelled explicitly, but does so within the framework of return-distribution modelling. We operate entirely within the PPP framework and identify the specific channels that forces conservatism without any distributional assumptions on returns. Our posterior is a Gibbs

posterior in the sense of [Bissiri et al. \(2016\)](#), updated by utility rather than likelihood, and PPP emerges as its mode under a flat prior.

Within the PPP literature, [Brandt et al. \(2009\)](#) and related work by [Brandt and Santa-Clara \(2006\)](#) treat θ as known with certainty throughout. Our contribution is to relax that assumption within the parametric policy-rule framework and quantify the portfolio implications of policy-parameter uncertainty. This is complementary to broader Bayesian portfolio-choice work such as [Garlappi et al. \(2007\)](#) and [Tu and Zhou \(2011\)](#) and others reviewed by [Avramov and Zhou \(2010\)](#), which operates in return-distribution or mean-variance allocation settings rather than PPP policy estimation. The result also complements work on portfolio regularisation ([DeMiguel et al., 2009](#); [Kojen et al., 2018](#)) by showing that shrinkage in PPP has a decision-theory interpretation rather than being only a statistical convenience. The paper also connects to the factor timing literature ([Haddad et al., 2020](#); [Ilmanen et al., 2021](#); [Arnott et al., 2019](#)) and the high-dimensional asset pricing literature ([Green et al., 2017](#); [Kozak et al., 2020](#); [Gu et al., 2020](#)). While those papers focus on signal selection in predicting the Stochastic Discount Factor, we look at the most relevant signals in the context of portfolio decisions by risk averse investors. Our utility-based approach also aligns with the critique in [Wang et al. \(2026\)](#), who argue that the conventional two-stage separation between return forecasting and portfolio optimisation is suboptimal. BPPP avoids that separation by design, directly optimising expected utility over the posterior distribution of policy parameters.

The remainder of the paper is organized as follows. Section 2 sets notation and motivates the exercise. Section 3 develops Bayesian Parametric Portfolio Policies and derives the key proposition; a brief discussion of the estimation procedure is provided at the end of that section, with full details in Appendix B. Section 4 describes the data. Section 5 presents empirical results. Section 6 reports robustness checks. Section 7 concludes.

2 Setup and Motivation

At each date t , an investor observes a vector of L signals z_t and chooses portfolio weights w_t over K assets. Portfolio returns realised at $t+1$ are $r_{p,t+1} = w_t' R_{t+1}$, where R_{t+1} is the vector of gross returns. The investor has time-separable CRRA preferences and, abstracting from intertemporal hedging motives, solves at each date t

$$\max_{w_t \in \mathcal{W}} \mathbb{E}_t[U(r_{p,t+1})], \quad (1)$$

where \mathcal{W} is the feasible set and $U(\cdot)$ is the utility function. Solving this problem directly requires the conditional distribution of $R_{t+1}|z_t$, which is high-dimensional and difficult to estimate reliably. [Brandt et al. \(2009\)](#) resolve this difficulty by restricting attention to portfolio rules that are explicit functions of observable signals. Weights follow the linear policy rule

$$w_t(\theta) = w_b + \theta z_t, \quad (2)$$

where w_b is a benchmark allocation (the market portfolio throughout) and $\theta \in \mathbb{R}^{K \times L}$ is the policy parameter matrix, normalised to portfolio-weight scale so that each entry $\theta_{k\ell}$ represents the weight response of asset k to signal ℓ , and θz_t is the signal-induced tilt away from the benchmark. In this framework, dynamic portfolio choice reduces to estimating θ . Given observations $\mathcal{D}_T = \{(R_{t+1}, z_t)\}_{t=1}^T$, the PPP investor solves

$$\hat{\theta} = \arg \max_{\theta} \frac{1}{T} \sum_{t=1}^T U(w_t(\theta)' R_{t+1}). \quad (3)$$

Equation 3 is a sample analogue of expected utility maximisation over policies, and it has three attractive properties. It delivers state-dependent, implementable portfolio rules, it requires no explicit return distribution, and it scales to large signal spaces.

The formulation of Parametric Portfolio Policies (PPP) treats the policy parameter θ

as an unknown but fixed object, estimated by maximising sample average utility. Once a point estimate $\hat{\theta}$ is obtained, portfolio decisions are taken as if this estimate were known with certainty. This plug-in approach is standard in the PPP literature, but it neglects estimation uncertainty in the policy parameters. From a decision-theory perspective, this omission is consequential. Policy parameters are estimated from a finite sample of noisy signals. When L is large relative to T , $\hat{\theta}$ is estimated with substantial error. Small perturbations in $\hat{\theta}$ translate linearly into portfolio tilts and can produce large, unstable weight changes from period to period. Excessive turnover and unstable portfolio choices are an expected consequence of estimation risk of PPP. The deeper issue, however, is not merely a finite-sample nuisance. The investor knows that θ is uncertain, yet behaves as if it is not. We formalise the cost of this inconsistency and propose another approach in the next section.

3 Bayesian Parametric Portfolio Policies

When θ is uncertain, rational portfolio choice requires integrating expected utility over this uncertainty rather than conditioning on a single estimated policy. We adopt a Bayesian perspective and treat the policy parameter θ as a random variable. Given a prior distribution $p(\theta)$ and the loss function implied by the PPP objective, the posterior distribution of θ is

$$p(\theta \mid \mathcal{D}_T) \propto \exp\left(\sum_{t=1}^T U(\pi(z_t; \theta)' R_{t+1})\right) p(\theta). \quad (4)$$

Rather than updating beliefs through a conventional likelihood, which would require a parametric model for returns, we follow [Bissiri et al. \(2016\)](#) and update using the PPP objective itself as a loss function. Under this formulation, the PPP estimator corresponds to the posterior mode under a flat prior. In contrast, Bayesian Parametric Portfolio Policies (BPPP) explicitly account for the full posterior distribution of θ . Given the posterior dis-

tribution $p(\theta \mid \mathcal{D}_T)$, the Bayesian investor evaluates portfolio performance by integrating expected utility over parameter uncertainty. Formally, the investor's objective at time t can be written as

$$\mathbb{E}_{\theta \mid \mathcal{D}_T} [\mathbb{E}_t [U(\pi(z_t; \theta)' R_{t+1})]],$$

integrating expected utility over both future returns and residual uncertainty about the policy. Portfolio weights are constructed as

$$w_t^{\text{BPPP}} = \mathbb{E}_{\theta \mid \mathcal{D}_T} [w_t(\theta)] = w_b + \mathbb{E}[\theta \mid \mathcal{D}_T] z_\tau, \quad (5)$$

where the last equality uses the linearity of $w_\tau(\theta)$ in θ . In practice, this expectation is approximated via a Laplace approximation averaging around the MAP policy (See Section B for further details). This construction highlights the key difference between PPP and BPPP. While PPP selects a single optimal policy and ignores estimation risk, BPPP averages over a distribution of plausible policies.

The Bayesian averaging implicit in BPPP has a clear economic interpretation which forms the basis of the central claim of this paper. Under nonlinear utility, expected utility is a concave function of portfolio returns. As a result, $U(\mathbb{E}[r_p]) \neq \mathbb{E}[U(r_p)]$, and ignoring parameter uncertainty can lead to overly aggressive portfolio choices. More precisely, under concave utility, expected utility is strictly less than the utility evaluated at expected returns. Parameter uncertainty therefore reduces expected utility even if it leaves expected returns unchanged. By integrating utility over the posterior distribution of policy parameters, BPPP internalizes estimation risk and produces more stable portfolio allocations. We formalize this result next.

Proposition 1 *Define the conditional expected utility of policy θ at date τ as*

$$G_\tau(\theta) = \mathbb{E}_\tau [U(w_\tau(\theta)' R_{\tau+1})],$$

and let $m_\tau = \mathbb{E}[\theta | \mathcal{D}_{T_\tau}]$ denote the posterior mean, $\Sigma_{\theta, \tau} = \text{Var}(\theta | \mathcal{D}_{T_\tau})$ the posterior covariance, U a strictly concave and twice continuously differentiable utility function, where $\Sigma_{\theta, \tau} \neq 0$. Then

$$\mathbb{E}_{\theta | \mathcal{D}_{T_\tau}}[G_\tau(\theta)] < G_\tau(m_\tau). \quad (6)$$

Moreover, to second order in $\Sigma_{\theta, \tau}$,

$$G_\tau(m_\tau) - \mathbb{E}_{\theta | \mathcal{D}_{T_\tau}}[G_\tau(\theta)] \approx -\frac{1}{2} \text{tr}(\nabla_\theta^2 G_\tau(m_\tau) \Sigma_{\theta, \tau}) > 0, \quad (7)$$

and under a quadratic approximation to U the difference is proportional to $z_\tau' \Sigma_{\theta, \tau} z_\tau$ and return second moments, hence strictly increasing in $\|z_\tau\|$ and in every eigenvalue of $\Sigma_{\theta, \tau}$.

The proof is in Appendix A. The proposition has three direct implications, each of which maps to an empirical prediction which forms the basis of our empirical exercise as follows.

(i) PPP overstates expected utility. The PPP investor evaluates $G_\tau(\hat{\theta}) \approx G_\tau(m_\tau)$ and treats this as the expected utility of the implemented policy. Inequality (6) says this number is always too high. The utility that will actually be achieved in expectation is $\mathbb{E}_\theta[G_\tau(\theta)] < G_\tau(m_\tau)$.

(ii) Overexposure is worst precisely when PPP bets hardest. From (7), the utility gap grows with $z_\tau' \Sigma_{\theta, \tau} z_\tau$, the quadratic form of posterior uncertainty evaluated at the current signal vector. When signals are large in magnitude, PPP generates large tilts *and* faces the largest utility overstatement. The two forces compound, i.e. PPP is most overconfident at exactly the moments it is most aggressive.

(iii) PPP underestimates portfolio risk. Under a mean-variance approximation, the investor's objective is $\mathbb{E}[r_{p, \tau+1}] - \frac{\gamma}{2} \text{Var}(r_{p, \tau+1})$. The law of total variance gives

$$\text{Var}(r_{p, \tau+1}) = \underbrace{\mathbb{E}_\theta[\text{Var}(r_{p, \tau+1} | \theta)]}_{\text{market risk}} + \underbrace{z_\tau' \Sigma_{\theta, \tau} z_\tau \cdot \|\mu_{\tau+1}\|^2}_{\text{estimation risk}}, \quad (8)$$

where $\mu_{\tau+1} = \mathbb{E}_{\mathcal{T}}[R_{\mathcal{T}} + 1]$ is the vector of conditional expected returns. The proof is in Appendix A. Notice that PPP ignores the second term. Ignoring parameter uncertainty is therefore equivalent to understating portfolio risk, and the resulting overexposure to signals is an arithmetic consequence of an incomplete objective. In implementation, PPP further approximates the first term using a plug-in policy at $\theta = m_{\tau}$. BPPP internalises the estimation-risk term by default, without any *ad hoc* penalty or constraint.

Two further observations follow directly from Proposition 1. First, the PPP investor solves for optimal policies under the assumption that posterior uncertainty is zero, i.e. $\Sigma_{\theta,\tau} = 0$. This is the certainty-equivalent approximation to the Bayesian decision rule. Proposition 1 quantifies the cost of this approximation, given by the estimation risk term in Equation 8, which grows without bound as L/T increases. In high-dimensional environments, the approximation error is largest.

Second, empirical gains associated to a BPPP ought to be largest for risk averse investors. Because the gap (7) scales with γ under quadratic approximation, the welfare cost of PPP is strictly increasing in risk aversion. A moderately risk-averse investor ($\gamma = 5$) suffers a utility overstatement proportional to $\frac{5}{2} z'_{\tau} \Sigma_{\theta,\tau} z_{\tau}$, while a highly risk-averse investor ($\gamma = 10$) suffers twice as much.

3.1 The role of the Prior

The prior $p(\theta)$ in equation (4) encodes the investor's *ex-ante* beliefs about how aggressively the policy should respond to signals. In this context, the prior summarises beliefs about the appropriate scale of portfolio tilts rather than a fully specified structural return model. It is worth noting that the prior also governs the posterior variance $\Sigma_{\theta,\tau}$ that determines the size of the utility gap in Proposition 1. Our baseline prior at time t is

$$\theta_t \sim \mathcal{N}(M_t, \nu I),$$

where M_t is the prior mean and ν is the effective prior variance. We set $M_t = \hat{\theta}_{t-1}$ so the prior penalises deviations from previous policy parameters, mimicking a regular rebalancing procedure by investors. The hyperparameter ν is set from a single economically interpretable quantity, the target-tilt standard deviation δ which defines the investor's prior belief about the typical magnitude of signal-induced deviations from M_t . With L standardised signals, the variance of the aggregate tilt on asset k is $L\sigma_\theta^2$, so setting the tilt's standard deviation to δ gives

$$\sigma_\theta = \frac{\delta}{\sqrt{L}}. \quad (9)$$

This calibration is dimension-adaptive.¹ As L grows, each individual coefficient is shrunk more tightly at rate $1/\sqrt{L}$, keeping the aggregate tilt stable. With $L = 242$ and $\delta = 0.35$, we obtain $\sigma_\theta \approx 0.0225$. To maintain a meaningful balance between prior and data as the estimation window expands, we scale the effective prior variance by $\max(T/L, 1)$

$$\nu = \sigma_\theta^2 \cdot \max\left(\frac{T}{L}, 1\right). \quad (10)$$

When $T \gg L$ the prior is diffuse and data dominate, whereas as $T \approx L$ the prior retains meaningful weight and prevents overfitting.

Horseshoe prior. The Gaussian prior shrinks all coefficients uniformly. In high-dimensional settings, predictability may instead be concentrated in a small number of signals with the majority being pure noise. To accommodate this possibility, we also estimate a variant using the regularised horseshoe prior of [Carvalho et al. \(2010\)](#) as refined by [Piironen and](#)

¹The numerical implementation stores θ at K times the portfolio-weight scale and computes tilts as $\tilde{\theta}_{z_t}/K$, so the variance of the aggregate tilt is $L\sigma_\theta^2/K^2$. Setting this equal to δ^2 gives $\sigma_\theta = K\delta/\sqrt{L}$ internally. Since $\theta = \tilde{\theta}/K$, the implied prior standard deviation on the portfolio-weight-scaled parameter is $\sigma_\theta = \delta/\sqrt{L}$ as stated, and the K factors cancel exactly in the MAP and Laplace computations.

[Vehtari \(2017\)](#) and defined as follows

$$\theta_{t,k,\ell} \mid \tilde{\lambda}_{t,k,\ell}, M_t \sim \mathcal{N}\left(M_{t,k,\ell}, \tilde{\lambda}_{t,k,\ell}^2\right), \quad (11)$$

$$\tilde{\lambda}_{t,k,\ell}^2 = \frac{c^2 \lambda_{t,k,\ell}^2 \tau^2}{c^2 + \lambda_{t,k,\ell}^2 \tau^2},$$

where τ is a global shrinkage scale, $\lambda_{t,k,\ell}$ are local scales, c is the slab scale of the Horseshoe, and σ^2 is residual variance. The global scale is calibrated as in [Piironen and Vehtari \(2017\)](#)

$$\tau_0 = \frac{p_0}{L - p_0} \frac{\sigma}{\sqrt{T}}, \quad (12)$$

with p_0 reflecting the prior expectation about the number of signals that carry genuine predictive content. The posterior shrinkage factor for each signal is

$$\kappa_{k,\ell} = \frac{1}{1 + \tilde{\lambda}_{k,\ell}^2 \|z_\ell\|^2 / \sigma^2},$$

where $\kappa \approx 0$ means the signal survives and $\kappa \approx 1$ means it is shrunk towards the mean. No coefficient is set exactly to zero, preserving the differentiable structure of the policy rule. [Table 1](#) summarises the two prior specifications used in the empirical exercise later.

Table 1: Summary of Prior Specifications

Model	Prior	Key hyperparameter	Shrinkage type
BPPP	$\mathcal{N}(M_t, \nu I)$	δ (target tilt SD)	Global, uniform
Horseshoe	$\mathcal{N}(M_t, \tilde{\lambda}^2)$	p_0 (expected signals)	Global-local, adaptive

Notes: ν is defined in Equation (10). $\tilde{\lambda}^2$ is the local scale from Equation (11). The Gaussian prior applies uniform shrinkage around $M_t = \hat{\theta}_{t-1}$. The horseshoe prior uses the same M_t but adapts shrinkage signal-by-signal through local scales.

The two priors span a spectrum of assumptions about signal sparsity. The Gaussian prior is appropriate when predictability is diffuse, the Horseshoe is appropriate when it is sparse. Comparing them empirically allows us to assess whether the gains from BPPP depend

on prior form or arise more broadly from posterior averaging. In this paper, we treat the Gaussian-vs-Horseshoe comparison as evidence on prior misspecification risk rather than a definitive model-selection result. Regardless of the prior chosen, none of these specifications impose hard constraints on the policy, perform variable selection in the frequentist sense, or alter the functional form of the decision rule. Their role is to determine the scale at which portfolio weights react to signals, controlled by Proposition 1’s $\Sigma_{\theta,\tau}$.

Given the posterior in Equation (4), portfolio weights are formed by averaging M draws of θ per Equation (5). Draws are obtained via a diagonal Laplace approximation centred at the maximum a posteriori (MAP) estimate, which is computed by L-BFGS-B optimisation of the penalised utility objective. The estimation window starts at $T_0 = 120$ months and grows recursively. At each step the prior mean is set to $M_t = \hat{\theta}_{t-1}$, so the prior anchors the new estimate to the previous period’s policy. The Horseshoe variant replaces the Gaussian prior update with a coordinate-ascent step over the local scales $\{\lambda_{k,\ell}\}$ and global scale τ . Full algorithmic details are in Appendix B.

4 Data

We use monthly returns on the six Fama–French factors. Market excess return (MKT-RF), size (SMB), value (HML), profitability (RMW), momentum (UMD), and investment (CMA), together with the one-month T-bill rate, downloaded from Professor Ken French’s Data Library. These form the investment universe ($K = 6$). The sample runs from July 1963 to December 2023.

As for predictive signals, we use 212 anomaly-based predictors drawn from the Open Source Asset Pricing database of [Chen and Zimmermann \(2022\)](#), constructed from CRSP and Compustat data and chosen for their replicability and breadth across the documented anomaly literature. The remaining 30 are factor-specific signals constructed following [Haddad et al. \(2020\)](#), covering time-series momentum, cross-sectional momentum, factor

valuation, reversal, and volatility for each factor. This combination of signal types ensures broad coverage of both firm-characteristic and factor-dynamics predictability.

Within each expanding estimation window, signals are standardised to zero mean and unit variance using only in-sample moments, ensuring no look-ahead bias. Missing values are replaced by zero after standardisation (mean imputation on the standardised scale). Predictors available at time t form portfolio weights at t , applied to returns realised at $t + 1$. We use an expanding window with an initial training sample of 120 months (1963M7–1973M7) and evaluate performance from 1973M8 onward, yielding 605 monthly out-of-sample observations (1973M8–2023M12). Portfolio rebalancing is monthly.

5 Empirical Results

Our empirical setting places the exercise squarely in the environment where Proposition 1 predicts the overexposure correction to be largest. We consider $L = 242$ signals and $K = 6$ assets consisting of the five [Fama and French \(2015\)](#) plus momentum factors, therefore deploying the Parametric Portfolio Policy framework of [Brandt et al. \(2009\)](#) in factor space. The empirical results are organised around the three predictions of Proposition 1, that PPP overstates achievable utility, that overexposure is worst when signals are strongest, and that the gap grows with risk aversion. We begin by comparing performance among methods over the full sample. Table 2 reports annualised out-of-sample statistics for all strategies. BPPP achieves a gross Sharpe ratio of 1.32 and PPP 1.05, both above the market benchmark (0.74), mean-variance portfolio (1.04), and simple momentum PPP strategy (0.93), which consists of PPP with a single momentum signal. As shown in Table 3, a circular block-bootstrap Sharpe-difference test rejects equal Sharpe ratios between BPPP and the market at the 1% level. PPP also outperforms significantly, but with lower precision, consistent with noisier coefficient estimates.

By integrating over the posterior distribution of θ , BPPP naturally shrinks extreme poli-

Table 2: Out-of-Sample Performance Comparison of Portfolio Strategies

	Mean (%)	Vol (%)	Sharpe	MaxDD (%)	VaR 95 (%)	CVaR 95 (%)	Turnover	Skew	Kurt.	Sharpe (net)
Benchmark (Mkt)	11.83	16.01	0.74	-50.31	-7.33	-10.11	0.00	-0.51	1.76	0.74
Mean-Variance	7.12	6.87	1.04	-15.74	-2.70	-4.44	0.39	-0.39	3.12	1.03
Simple Mom	8.93	9.57	0.93	-31.67	-4.16	-5.95	1.26	-0.49	2.40	0.92
PPP	11.15	10.64	1.05	-37.21	-3.76	-6.09	9.54	0.30	5.37	0.96
BPPP	12.18	9.24	1.32	-24.50	-3.28	-4.85	6.03	-0.11	1.39	1.25
Horseshoe	12.18	10.36	1.18	-23.20	-3.93	-5.86	5.55	-0.18	2.06	1.12

Notes: Expanding window, initial training sample 120 months (1963M7), out-of-sample period 1973M8–2023M12. Mean and volatility are annualised. MaxDD is maximum drawdown. VaR and CVaR at 95% denote Value-at-Risk and Conditional Value-at-Risk (Expected Shortfall). Turnover is average one-way per period. Sharpe (net) deducts 10 bps transaction costs per unit of one-way turnover.

cies, dampens the effect of noisy predictors, and produces smoother portfolio dynamics. These effects are particularly pronounced in finite samples and in the presence of portfolio constraints, where estimation error can otherwise translate into excessive turnover and poor downside performance. Importantly, BPPP does not alter the underlying economic signals or the functional form of the policy rule. Instead, it modifies how uncertainty about the policy parameters is incorporated into decision making. In this sense, BPPP represents a principled extension of the PPP framework rather than an alternative modelling approach.

Proposition 1 predicts that PPP overreacts to signals, and this is most visible in turnover. PPP generates average one-way turnover of 9.54 per period, the highest of any active strategy. BPPP reduces this to 6.03 and horseshoe to 5.55. At 10 basis points per unit of one-way turnover, PPP’s net Sharpe falls from 1.05 to 0.96, while BPPP’s falls only from 1.32 to 1.25. At 50 basis points, PPP collapses to 0.60 while BPPP remains near 0.99.

The turnover difference reflects the mechanism of Proposition 1 directly. Because $\Sigma_{\theta,\tau}$ is non-negligible relative to T/L , BPPP shrinks tilts in the direction of high signal magnitude. This prevents the over-reaction to large signal realisations that drives PPP’s excessive position changes. Figure 1 confirms this at the factor level. PPP tilts chase signals, generating high weight volatility. BPPP maintains a more balanced factor exposure and

markedly lower time-series weight volatility across all six factors. The return distribution (Figure A1, left panel) reflects this. PPP exhibits positive skewness (0.30) and heavy kurtosis (5.37) consistent with episodic overexposure, whereas BPPP is near-symmetric (-0.11) with lighter tails (Kurtosis of 1.39).

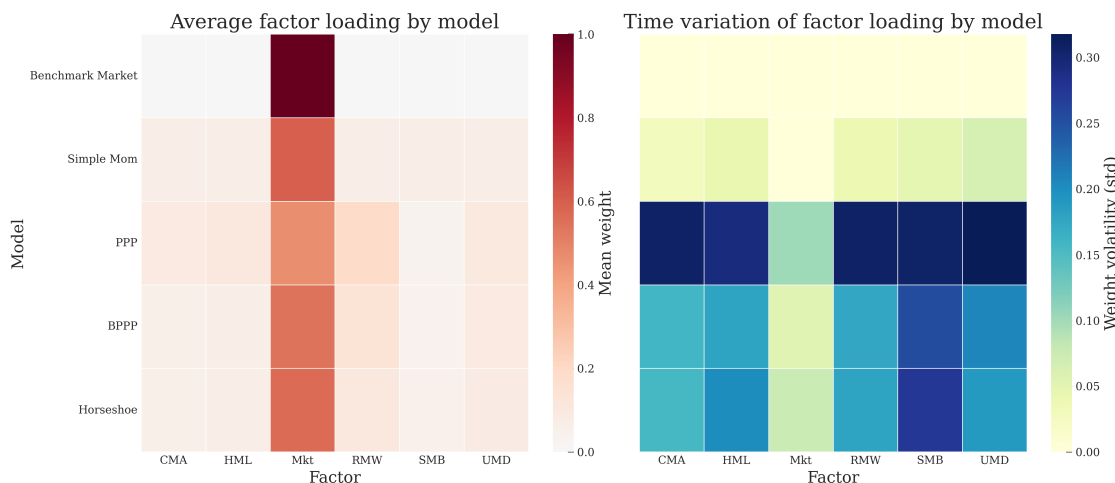


Figure 1: Factor Exposures by Model

Notes: Left: average portfolio weight on each factor. Right: time-series standard deviation of factor weights. BPPP exhibits substantially lower weight volatility across all factors, consistent with the overexposure correction predicted by Proposition 1.

The mechanism operates at the signal level as well as the factor level. Appendix Figures A6–A8 display heatmaps of the largest signal–factor coefficient pairs by absolute magnitude across PPP, BPPP, and the Horseshoe. Two patterns emerge. First, all three models draw on a common pool of predictive signals. Momentum-related signals from Haddad et al. (2020) and valuation-based anomalies from Chen and Zimmermann (2022) consistently rank among the most influential across specifications, suggesting that the predictive information in the signal set has systematic structure that each method detects. Second, the scale and dispersion of the largest coefficients differ markedly across methods. PPP concentrates weight on a small number of extreme loadings, a direct reflection of the overfit that Proposition 1 attributes to ignoring $\Sigma_{\theta, \tau}$. BPPP distributes weight more evenly, posterior averaging dilutes the contribution of any single signal realisation, shrinking extreme coefficients without eliminating them. The Horseshoe achieves the most aggressive reg-

ularization of large coefficients through its signal-specific local scales, yet, as we discuss below, without inducing the sparsity its design assumes.

The evidence bears directly on the sparse vs. dense debate in the return predictability literature (Kozak et al., 2020; Gu et al., 2020) and by . Under a sparse model, a small number of signals would carry all predictive information and the remainder would be driven to zero. The horseshoe shrinkage factor κ is designed precisely to discriminate signals, i.e. $\kappa_{k,\ell} \approx 0$ indicates a surviving signal; $\kappa_{k,\ell} \approx 1$ indicates collapse toward the prior mean. Figure A5 shows that the empirical κ distribution is concentrated near zero throughout the out-of-sample period (final OOS mean ≈ 0.03 , median ≈ 0.02 , with 99.6% of coefficients below 0.3). This evidence suggests *dense* predictability, the horseshoe finds no evidence for a small dominant subset of signals. Instead, broad signal ‘survival’ characterises the data. The bootstrap stability analysis of Figure A9 reinforces this conclusion. Drawing 500 random subsets of 50 signals from the full 242, the distribution of mean absolute horseshoe coefficients is tightly concentrated, confirming that no small cluster of signals is the primary performance driver. This is consistent with Kozak et al. (2020) and Haddad et al. (2020), who argue that factor timing predictability reflects a diffuse combination of many signals rather than a sparse set of dominant predictors. In this environment, the Gaussian prior’s uniform shrinkage is better matched to the structure of the data than the horseshoe’s sparsity assumption, which helps explain BPPP’s outperformance of the horseshoe in our sample. The relative performance of the two prior specifications is therefore informative beyond portfolio statistics. It constitutes out-of-sample evidence on the density structure of return predictability in factor timing.

Next, Proposition 1 identifies the welfare cost of PPP as the utility gap $G_\tau(m_\tau) - \mathbb{E}_\theta[G_\tau(\theta)]$. The empirical counterpart of this gap is the difference of certainty-equivalents. Table A1 reports CE returns under CRRA utility with $\gamma = 5$. BPPP delivers an annualised CE of 10.52%, corresponding to a difference of 536 basis points relative to the market benchmark. PPP delivers a CE of 8.68%. The 184 basis point gap between BPPP and PPP in CE space

is the empirical counterpart of the utility overstatement that Proposition 1 predicts. Empirical CE is computed using the exact CRRA transformation, whereas Proposition 1 uses a second-order mean-variance approximation; the correspondence is therefore economic rather than algebraically exact.

Figure A2 maps all strategies in risk-return space. BPPP occupies the north-west of the frontier, combining higher return and lower volatility than PPP and the market benchmark. Figure A3 shows cumulative wealth over the full out-of-sample period. With respect to tail risk, the maximum drawdown of PPP (-37.2%) is substantially larger than that of BPPP (-24.5%). This is a direct consequence of overexposure. PPP holds extreme positions precisely when signals are anomalously large, and these are often periods of elevated market stress when large tilts carry the greatest downside. BPPP's posterior averaging dampens the response to extreme signal realisations, providing asymmetric protection against tail events. Notwithstanding, tail risk as measured by Value-at-Risk is not substantially higher. The spanning regressions in Table 4 confirm that BPPP generates higher benchmark-orthogonal value. Alpha is 6.86% versus 6.53% for PPP, with higher R^2 (0.61 vs. 0.35), indicating that BPPP maintains meaningful market exposure while adding alpha more efficiently.

6 Robustness

This section is organized around five lines of enquiry. First, are performance statistics, in particular risk-adjusted returns of different methods statistically significant and do they represent genuine alpha? Second, is the welfare advantage of BPPP monotonically increasing in risk aversion as Proposition 1 predicts? Third, does the performance gap survive realistic transaction costs? Fourth, is subperiod performance consistent or driven by a episodic differences? Finally, are results sensitive to prior choices and specification.

6.1 Statistical Significance and Spanning Tests

A first concern is whether the performance gap between BPPP and benchmarks reported in Table 2 is a statistical artefact of the specific sample choice. We address this with a bootstrap Sharpe-difference test and a market-spanning regression. Table 3 reports Sharpe-difference tests against the market benchmark following [Ledoit and Wolf \(2008\)](#). Under this procedure, BPPP rejects the null of equal Sharpe ratio at the 1% level with a t -statistic of 5.61. The Horseshoe is also strongly significant ($t = 4.18$). PPP is significant at the 5% level ($t = 2.34$) but with a bootstrap standard error roughly 30% larger than BPPP’s, reflecting the higher sampling variability of its coefficients when estimation risk is ignored. The mean-variance strategy attains marginal significance ($t = 1.99$).

Table 3: Bootstrap Sharpe-Difference Tests vs. Market Benchmark

Portfolio	Sharpe Diff	Bootstrap SE	t -stat	p -value
BPPP	0.579	0.103	5.61	<0.001***
Horseshoe	0.437	0.105	4.18	<0.001***
PPP	0.309	0.132	2.34	0.019**
Mean-Var	0.297	0.149	1.99	0.047**

Notes: Null hypothesis: Sharpe ratio equals that of the market. Studentised bootstrap test of [Ledoit and Wolf \(2008\)](#) with block length $\lfloor T^{1/3} \rfloor = 8$ months. ***, **, *: significant at 1%, 5%, 10%.

The pairwise BPPP vs. PPP Sharpe gap of 0.27 is directionally positive but measured with substantial noise, as both strategies exploit the same signal set and factor universe. The BPPP advantage over PPP reflects a difference in how parameter uncertainty is handled, not access to a fundamentally different information set.

Table 4 sharpens the interpretation via OLS regressions of excess returns on the market. BPPP generates an annualised alpha of 6.86% ($t = 8.20$), above PPP’s 6.53% ($t = 5.27$). Two contrasts stand out. First, BPPP’s alpha t -statistic is 56% larger than PPP’s despite very similar point estimates. The posterior averaging reduces residual volatility, making the alpha estimate much more precise. Second, BPPP has a higher market beta (0.45 versus 0.39 for PPP) and substantially higher R^2 (0.61 versus 0.35). This combination (higher sys-

Table 4: Spanning Tests: Alpha and Beta vs. Market Benchmark

Portfolio	α (ann. %)	β	t -stat	p -value	R^2
PPP	6.53	0.39	5.27	<0.001***	0.35
BPPP	6.86	0.45	8.20	<0.001***	0.61
Mean-Var	4.26	0.24	5.20	<0.001***	0.32
Horseshoe	6.44	0.48	6.52	<0.001***	0.56

Notes: OLS regression of model excess returns on market excess return. Alpha annualised. t -stats and p -values for $H_0 : \alpha = 0$.

tematic loading with lower residual variance) indicates that BPPP builds market exposure more deliberately. PPP’s lower R^2 reflects the idiosyncratic noise introduced by extreme coefficient estimates that BPPP’s prior dampens. Crucially, BPPP’s outperformance is not achieved by tilting away from market risk. It reflects the more efficient construction of factor tilts around a stable market factor.

6.2 Welfare and Risk-Aversion Analysis

One of Proposition 1 predictions is that the utility gap between BPPP and PPP should grow monotonically with γ because the Jensen’s inequality bound in Equation (7) scales linearly with risk aversion under a quadratic approximation (see Appendix A for more details). Table 5 provides a direct out-of-sample test.

Table 5: Certainty-Equivalent Returns Under Alternative Risk Aversion

	$\gamma = 2$	$\gamma = 5$	$\gamma = 10$
PPP	10.51	8.68	5.58
BPPP	11.94	10.52	8.13
Horseshoe	11.69	9.90	6.82
Benchmark	9.62	5.15	-2.94

Notes: Annualised CE returns (%) under exact CRRA utility with risk aversion γ . Consistent with Proposition 1, the BPPP advantage over PPP is monotonically increasing in γ .

The evidence strongly confirms the proposition. At $\gamma = 2$ the BPPP–PPP CE gap is 142 basis points annually (11.94% versus 10.51%). At $\gamma = 5$ it rises to 184 basis points (10.52% versus 8.68%). At $\gamma = 10$ it reaches 255 basis points (8.13% versus 5.58%). The

monotone increase is out-of-sample evidence of the overexposure mechanism. As risk aversion rises, the investor weights large negative returns more heavily under the concave utility function, and PPP's tendency to hold extreme positions exactly during high-signal-magnitude periods carries an increasingly large welfare cost. The Horseshoe lies between BPPP and PPP at all levels of γ , consistent with its intermediate degree of overexposure correction.

The benchmark CE trajectory is equally instructive. At $\gamma = 2$ the benchmark delivers a CE of 9.62%, below PPP's 10.51%. By $\gamma = 10$, benchmark CE collapses to -2.94% . Passive factor exposure destroys welfare because the variance penalty swamps the expected return. This provides context for interpreting the BPPP advantage under institutional risk aversion ($\gamma = 5-10$). The active correction for estimation risk is not a marginal refinement but a welfare-determining design choice. At $\gamma = 5$, the performance fee that a benchmark investor would pay to switch to BPPP is 500 basis points per annum (Table A1 in the appendix), compared with 331 basis points for PPP. The 169 basis-point fee difference is the monetary equivalent of the estimation-risk correction in our sample.

6.3 Transaction Costs and Trading Frictions

The turnover advantage of BPPP translates directly into a transaction-cost advantage that widens as frictions increase. Figure 2 plots net Sharpe ratios for all strategies against one-way transaction costs from 0 to 50 basis points.

At zero cost, BPPP leads PPP by 0.27 Sharpe points (1.32 versus 1.05). Far from narrowing with cost, the gap expands. At 10 bps the difference is 0.29 (1.25 versus 0.96), at 20 bps it is 0.32 (1.19 versus 0.87), at 50 bps it is 0.39 (0.99 versus 0.60). The BPPP-PPP gap is therefore strictly increasing in transaction costs, which is not mechanical. The posterior averaging that corrects overexposure simultaneously reduces the sensitivity of portfolio weights to noisy signal fluctuations, generating more persistent positions and lower rebalancing frequency. The cost advantage is a direct consequence of the same mechanism,

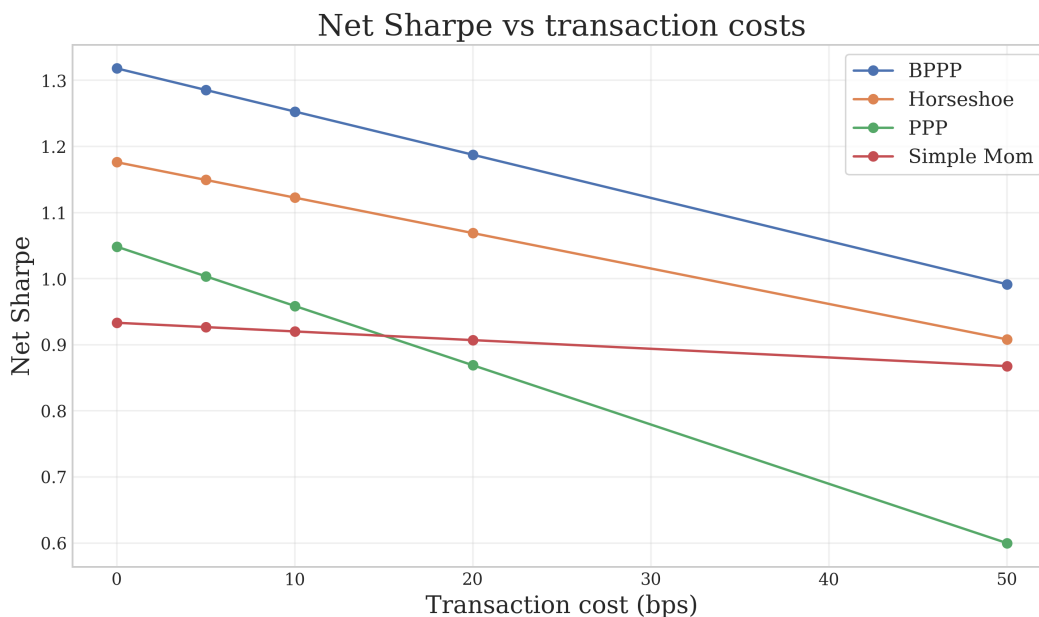


Figure 2: Net Sharpe Ratio vs. Transaction Costs

Notes: Net Sharpe ratios as a function of one-way transaction costs (0–50 bps).

reduced overreaction, that generates the gross Sharpe advantage.

For BPPP, the breakeven transaction cost at which the Sharpe falls below the market benchmark’s 0.74 exceeds 50 basis points, i.e., above the full 0–50 bps grid we test. For the Horseshoe, which has even lower turnover (5.55), the breakeven is similarly high.

6.4 Subperiod Stability and Crisis Resilience

A second concern is whether results are over-reliant on a few fortuitous subperiods. We assess this along two dimensions. Decade-by-decade analysis and crisis-episode analysis.

Figure 3 reports Sharpe ratios by decade. BPPP outperforms PPP in four of the five complete decades. The first decade (1973–1982) is the sole exception, with BPPP Sharpe of 0.98 versus PPP’s 0.99, a negligible margin of 0.003 Sharpe points consistent with sampling variation. In all subsequent decades the advantage is unambiguous. The equity bull market of the 1980s, the technology boom and bust of the 1990s, the post-GFC recovery of the 2000s, and the most recent decade. The advantage is largest in the 2003–2012 decade,

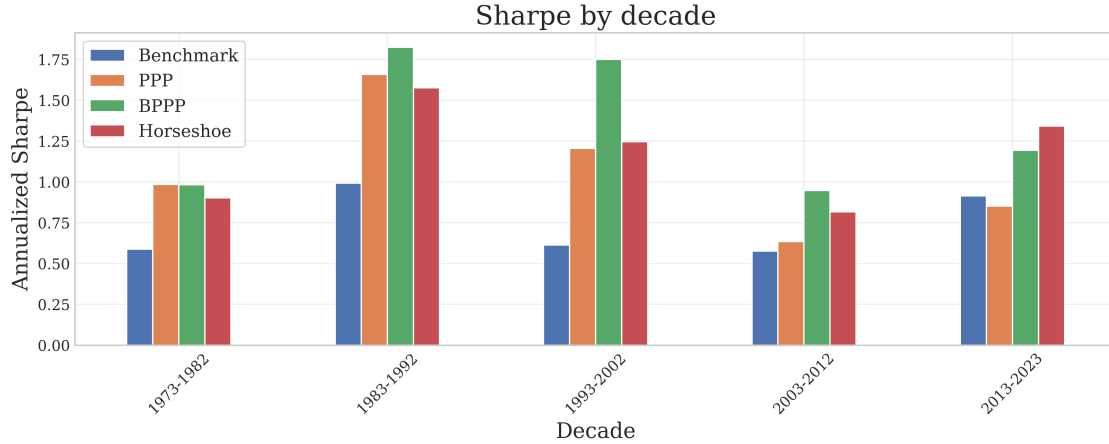


Figure 3: Sharpe Ratios by Decade

Notes: Annualised Sharpe ratios by complete out-of-sample decade. BPPP outperforms PPP in four of five complete decades. First decade (1963–1972) excluded as it overlaps with the in-sample training window.

spanning the Global Financial Crisis, precisely the period where Proposition 1 predicts the largest cost of ignoring $\Sigma_{\theta, \tau}$. Signals were anomalously large and volatile, PPP loaded heavily on them, and the result was the deep drawdown (-37.2%) that BPPP avoided (-24.5%). Across complete decades, BPPP outperforms the market benchmark in all five, while PPP underperforms the benchmark in the most recent decade (2013–2023), confirming that factor timing adds value on average and that the BPPP correction improves robustness over time.

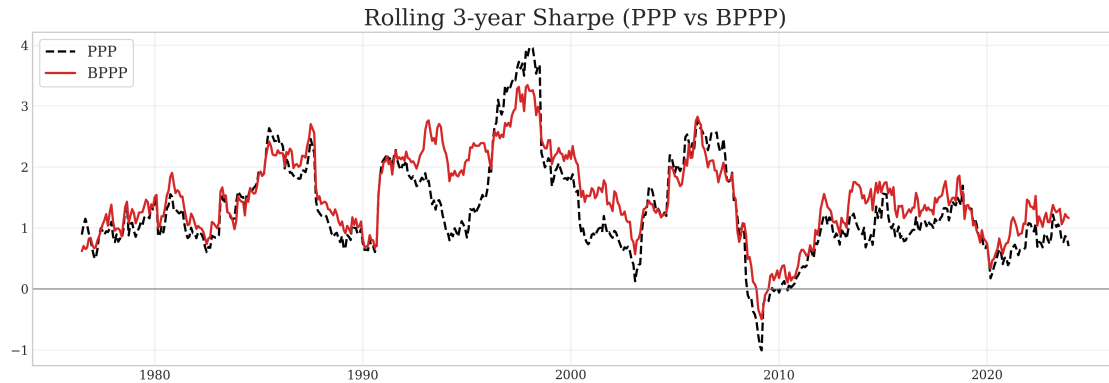


Figure 4: Rolling 36-Month Sharpe Ratios

Notes: Rolling 36-month Sharpe ratios, 1973M8–2023M12. PPP (black dashed); BPPP (red solid).

Figure 4 shows rolling 36-month Sharpe ratios. In calm periods, BPPP and PPP track

each other closely. When signals are moderate and estimation error has limited portfolio impact, posterior averaging introduces little change relative to the plug-in estimator. During stress episodes, however, the divergence is pronounced. Both the early-2000s technology correction and the 2008–2009 financial crisis show BPPP maintaining substantially higher rolling Sharpe than PPP. This asymmetry, better performance in bad times, near parity in good times, is evidence of the mechanism in Proposition 1. The Jensen’s inequality gap scales with $z_{\tau}'\Sigma_{\theta,\tau}z_{\tau}$, which is largest when signal magnitudes are extreme, and extreme signal episodes disproportionately coincide with financial crises.

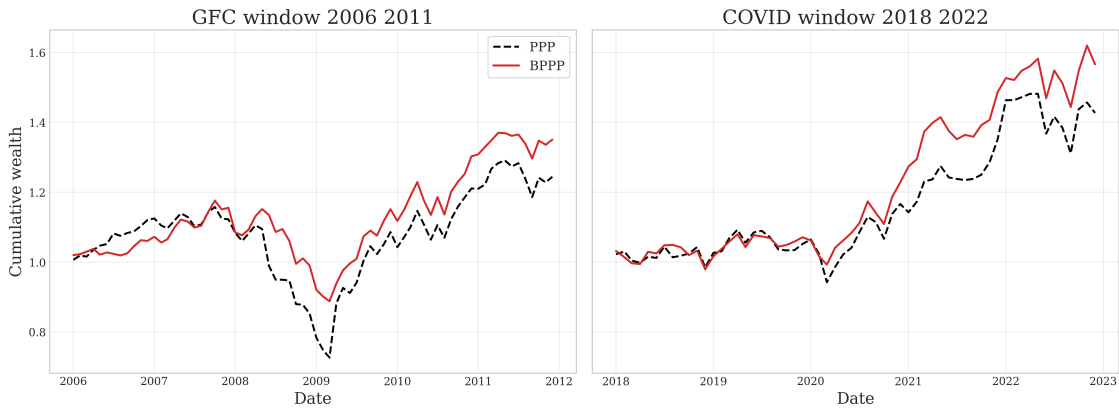


Figure 5: Cumulative Wealth During Crisis Episodes

Notes: Cumulative portfolio wealth during the GFC (left, 2006–2011) and COVID (right, 2018–2022). PPP (black dashed); BPPP (red solid).

Figure 5 zooms into the two major crisis episodes. During the GFC window (2006–2011), BPPP achieves a Sharpe of 0.56 versus 0.33 for PPP, a 71% relative improvement with a materially smaller drawdown. The GFC is a particularly demanding test because factor signal dispersion was unusually high in the pre-crisis period and PPP loaded aggressively on those signals. BPPP’s posterior averaging compressed the tilts, preventing the losses that large leveraged factor positions incurred as the crisis unfolded. During the COVID shock (2018–2022), BPPP leads with 0.89 versus 0.66. The COVID episode differs in character. The signal dislocation was sharper but more transient. The BPPP advantage here reflects faster mean-reversion of portfolio weights after the initial shock, consistent with the reduced sensitivity to large individual signal realisations that posterior averaging

produces.

The drawdown profile (Figure A4 in the appendix) confirms the picture at the path level. BPPP's maximum drawdown of -24.5% is 12.7 percentage points smaller than PPP's -37.2%, and the recovery from the 2008 trough is faster. The normal Q-Q plot in the same figure shows PPP's return distribution has materially heavier left tails than the normal, while BPPP's tails are near-Gaussian, consistent with the excess kurtosis of 1.39 versus 5.37 for PPP reported in Table 2. Together, the crisis and drawdown evidence confirms the third implication of Proposition 1, that PPP systematically understates portfolio risk via the estimation-risk term in Equation (8), and the downside consequences are concentrated in exactly the episodes where estimation risk is most consequential.

6.5 Prior Sensitivity and Dynamic Prior Mean

The BPPP framework requires two specification choices. The target-tilt standard deviation δ , which governs prior tightness, and whether the prior mean is set dynamically ($M_t = \hat{\theta}_{t-1}$) or held fixed at zero ($M_t = 0$), an alternative and legitimate choice. Table 6 reports the full sensitivity grid across $\delta \in \{0.35, 0.50, 0.70, 0.90\}$ with both prior-mean settings. The range spans from a tight prior ($\delta = 0.35, \nu \approx 0.0015$) to a loose one ($\delta = 0.90, \nu \approx 0.010$), a roughly sevenfold increase in prior variance.

Sensitivity to prior tightness (δ). Across the static specification, Sharpe ratios range from 1.032 to 1.147 as δ varies from 0.70 to 0.35, a variation of less than 0.12 over a sevenfold change in prior variance. CE returns span 6.6% to 8.2%. The insensitivity is structural. As δ rises from 0.35 to 0.90, mean $|\theta|$ nearly doubles (0.010 to 0.015) and tilt norms also rise. Once the constraints bind regularly, loosening the prior buys coefficient freedom that the portfolio construction step absorbs without converting to proportionally larger active positions. This insensitivity is reassuring since within a broad range, the prior-tightness choice does not materially change the results.

Table 6: BPPP Prior Sensitivity Study

δ	Dynamic M_t	Sharpe	CE (%)	Turnover	Mean tilt norm	Mean $ \theta $
0.35	No	1.147	8.205	3.76	0.567	0.0105
0.35	Yes	1.318	10.517	6.03	0.661	0.0263
0.50	No	1.053	7.025	2.31	0.536	0.0137
0.50	Yes	1.313	9.850	5.24	0.640	0.0346
0.70	No	1.032	6.645	1.63	0.544	0.0144
0.70	Yes	1.308	9.418	4.56	0.627	0.0418
0.90	No	1.055	6.688	1.46	0.557	0.0146
0.90	Yes	1.288	9.050	4.21	0.626	0.0518

Notes: BPPP sensitivity across target-tilt standard deviation δ and dynamic-prior-mean setting. “Dynamic M_t ” sets the prior mean to the previous period’s MAP estimate. Turnover is annualised one-way. Mean $|\theta|$ and mean tilt norm are structural diagnostics.

The role of the dynamic prior mean. The dynamic prior mean ($M_t = \hat{\theta}_{t-1}$) has a first-order effect across every value of δ . Switching from static to dynamic adds approximately 0.17–0.28 Sharpe points and 2.3–2.8 percentage points of annualised CE. At the baseline $\delta = 0.35$, the dynamic prior increases Sharpe from 1.147 to 1.318 and CE from 8.2% to 10.5%. This is the largest single performance differential in the sensitivity grid, larger than any choice of δ within either specification.

The economic mechanism is important to understand. When $M_t = \hat{\theta}_{t-1}$, the prior penalises deviations from the investor’s recent coefficient estimate rather than from zero. This anchors each period’s MAP to the previous solution, providing coefficient-level inertia that complements the posterior averaging over policy uncertainty. Specifically, it prevents the MAP from jumping to an extreme solution when a new data point arrives with anomalously large signals, because the prior cost of moving far from $\hat{\theta}_{t-1}$ is substantial. The result is lower within-period coefficient volatility and smoother portfolio dynamics over time.

The apparent paradox, that turnover is *higher* under the dynamic prior (6.03) than the static one (3.76) at $\delta = 0.35$, resolves on inspection. The static prior ($M_t = 0$) strongly attracts the MAP toward the origin in every period, compressing all tilts toward the benchmark and limiting the model’s ability to maintain persistent non-zero positions. The dy-

dynamic prior allows the MAP to track a slowly evolving signal environment, maintaining persistent tilts that accumulate across periods. These persistent tilts imply higher coefficient magnitude, higher tilt norms, and higher one-way turnover as positions are adjusted at each rebalancing date. The static specification's lower turnover therefore reflects over-shrinkage toward zero, a conservative stance that sacrifices the information in persistent signals, rather than efficient portfolio allocation. The CE gap of over 2 percentage points per annum documents the welfare cost of that conservatism.

Horseshoe prior specification. As discussed in Section 5, the horseshoe's underperformance relative to BPPP (Sharpe 1.18 versus 1.32) reflects a prior misalignment. The κ distribution is concentrated near zero throughout the out-of-sample period, indicating that broad signal survival (not sparse selection) characterises the data. The horseshoe's sparsity assumption is at odds with the dense predictability structure documented in the signal-level analysis, and the Gaussian prior is the better-calibrated specification for this environment. We treat the prior comparison as empirical evidence on the structure of factor-timing predictability rather than a definitive finding about priors in general, settings with genuinely sparse predictability could favour the horseshoe.

7 Conclusion

Parametric Portfolio Policies offer a powerful and flexible framework for dynamic asset allocation, but ignore policy uncertainty. Our key proposition formalises the consequences and shows that, because portfolio weights are linear in policy parameters and utility is concave, PPP systematically overstates achievable expected utility by an amount proportional to parameter uncertainty and signal scale. The correction is not a heuristic. It follows from Jensen's inequality applied to the posterior distribution of policy parameters.

Bayesian Parametric Portfolio Policies implement a corrected decision rule by integrating expected utility over this posterior. The correction arises by default, requiring no addi-

tional modelling of returns, and adds negligible computational cost. The prior controls the scale of posterior uncertainty and the degree of overexposure correction. Tighter priors impose larger corrections, translating into lower turnover and more stable weights.

Our empirical results confirm each prediction of the theory. BPPP delivers a gross Sharpe ratio of 1.32 versus 1.05 for PPP and 0.74 for the market. The certainty-equivalent difference is 536 basis points (BPPP) versus 353 basis points (PPP), a 184 basis point premium that represents the empirical counterpart of the utility overstatement in our key proposition. The gap grows with risk aversion, is largest during crisis episodes, and remains strong across decades (BPPP leads PPP in four of five complete decades). At 50 basis points of transaction costs, BPPP retains a net Sharpe of 0.99 while PPP collapses to 0.60.

A further finding is that the structure of predictability in factor timing appears diffuse rather than sparse. Most of the 242 signals are not strongly shrunk and appear to contribute jointly in our sample, favouring uniform Gaussian shrinkage over the horseshoe's sparse-signal design. We treat this as robust empirical evidence for this setting, while leaving broader prior-selection comparisons to future work.

Several extensions are natural. Replacing the isotropic Gaussian prior with a structured prior that accounts for cross-signal correlations would allow for more targeted overexposure correction in directions of high uncertainty. Extending BPPP to individual equities would test scalability at much larger K . Sequential Bayesian updating across windows would allow the posterior to adapt to structural breaks in factor dynamics without restarting from scratch.

References

- Arnott, R. D., Harvey, C. R., Kalesnik, V., and Linnainmaa, J. T. (2019). Alice's adventures in factorland: Three blunders that plague factor investing. *The Journal of Portfolio Management*, 45(4):18–36.
- Avramov, D. and Zhou, G. (2010). Bayesian portfolio analysis. *Annual Review of Financial Economics*, 2(1):25–47.
- Barberis, N. (2000). Investing for the long run when returns are predictable. *The Journal of Finance*, 55(1):225–264.
- Bissiri, P. G., Holmes, C. C., and Walker, S. G. (2016). A general framework for updating belief distributions. *Journal of the Royal Statistical Society: Series B (Statistical Methodology)*, 78(5):1103–1130.
- Brandt, M. W. and Santa-Clara, P. (2006). Dynamic portfolio selection by augmenting the asset space. *The Journal of Finance*, 61(5):2187–2217.
- Brandt, M. W., Santa-Clara, P., and Valkanov, R. (2009). Parametric portfolio policies: Exploiting characteristics in the cross-section of equity returns. *Review of Financial Studies*, 22(9):3411–3447.
- Carvalho, C. M., Polson, N. G., and Scott, J. G. (2010). The horseshoe estimator for sparse signals. *Biometrika*, 97(2):465–480.
- Chen, A. Y. and Zimmermann, T. (2022). Open source cross-sectional asset pricing. *Critical Finance Review*, 27(2):207–264. Data available at <https://www.openassetpricing.com/>.
- DeMiguel, V., Garlappi, L., and Uppal, R. (2009). Optimal versus naive diversification: How inefficient is the 1/N portfolio strategy? *The Review of Financial Studies*, 22(5):1915–1953.
- Fama, E. F. and French, K. R. (2015). A five-factor asset pricing model. *Journal of Financial Economics*, 116(1):1–22.
- Garlappi, L., Uppal, R., and Wang, T. (2007). Portfolio selection with parameter and model uncertainty: A multi-prior approach. *The Review of Financial Studies*, 20(1):41–81.

- Green, J., Hand, J. R. M., and Zhang, X. F. (2017). The characteristics that provide independent information about average U.S. monthly stock returns. *The Review of Financial Studies*, 30(12):4389–4436.
- Gu, S., Kelly, B., and Xiu, D. (2020). Empirical asset pricing via machine learning. *The Review of Financial Studies*, 33(5):2223–2273.
- Haddad, V., Kozak, S., and Santosh, S. (2020). Factor timing. *The Review of Financial Studies*, 33(5):1980–2018.
- Ilmanen, A., Israel, R., Moskowitz, T. J., Thapar, A. K., and Wang, F. (2021). Factor premia and factor timing: A century of evidence. *Journal of Alternative Investments*, 24(3):5–24.
- Kandel, S. and Stambaugh, R. F. (1996). On the predictability of stock returns: An asset-allocation perspective. *The Journal of Finance*, 51(2):385–424.
- Koijen, R. S. J., Moskowitz, T. J., Pedersen, L. H., and Vrugt, E. B. (2018). Carry. *Journal of Financial Economics*, 127(2):197–225.
- Kozak, S., Nagel, S., and Santosh, S. (2020). Shrinking the cross-section. *Journal of Financial Economics*, 135(2):271–292.
- Ledoit, O. and Wolf, M. (2008). Robust performance hypothesis testing with the Sharpe ratio. *Journal of Empirical Finance*, 15(5):850–859.
- Pástor, Ľ. and Stambaugh, R. F. (2000). Comparing asset pricing models: An investment perspective. *Journal of Financial Economics*, 56(3):335–381.
- Piironen, J. and Vehtari, A. (2017). Sparsity information and regularization in the horseshoe and other shrinkage priors. *Electronic Journal of Statistics*, 11(2):5018–5051.
- Tu, J. and Zhou, G. (2011). Markowitz meets talmud: A combination of sophisticated and naive diversification strategies. *Journal of Financial Economics*, 99(1):204–215.
- Wang, Y., Gao, H., Harvey, C. R., Liu, Y., and Tao, X. (2026). Machine learning meets Markowitz. Working Paper 34861, National Bureau of Economic Research.

A Proofs and Additional Details

Proof of Proposition 1

We prove the two claims in turn.

Part 1: Jensen's inequality bound (Equation 6).

Recall that portfolio weights are linear in θ :

$$w_\tau(\theta) = w_b + \theta z_\tau,$$

so the portfolio return $r_{p,\tau+1}(\theta) = w_\tau(\theta)' R_{\tau+1}$ is linear in θ for any fixed $(z_\tau, R_{\tau+1})$. We define

$$G_\tau(\theta) = \mathbb{E}_\tau[U(w_\tau(\theta)' R_{\tau+1})],$$

where the expectation is taken over the distribution of $R_{\tau+1}$ conditional on information at τ . Because $r_{p,\tau+1}(\theta)$ is linear in θ and U is strictly concave, $G_\tau(\theta)$ is strictly concave in θ . Thus, applying Jensen's inequality to the concave function $G_\tau(\cdot)$ and the posterior distribution $p(\theta \mid \mathcal{D}_{T_\tau})$ yields

$$\mathbb{E}_{\theta \mid \mathcal{D}_{T_\tau}}[G_\tau(\theta)] \leq G_\tau(\mathbb{E}_{\theta \mid \mathcal{D}_{T_\tau}}[\theta]) = G_\tau(m).$$

Since U is *strictly* concave and $\Sigma_\theta \neq 0$, the inequality is strict

$$\mathbb{E}_{\theta \mid \mathcal{D}_{T_\tau}}[G_\tau(\theta)] < G_\tau(m). \quad \blacksquare$$

Part 2: Second-order approximation (Equation 7).

Take a second-order Taylor expansion of $G_\tau(\theta)$ around $\theta = m$ which returns

$$G_\tau(\theta) \approx G_\tau(m) + \nabla_\theta G_\tau(m)' \text{vec}(\theta - m) + \frac{1}{2} \text{vec}(\theta - m)' \nabla_\theta^2 G_\tau(m) \text{vec}(\theta - m).$$

Taking expectations over the posterior $p(\theta \mid \mathcal{D}_T)$ yields

$$\begin{aligned}\mathbb{E}_{\theta \mid \mathcal{D}_T}[G_\tau(\theta)] &\approx G_\tau(m) + \nabla_\theta G_\tau(m)' \underbrace{\mathbb{E}[\text{vec}(\theta - m)]}_{=0} + \frac{1}{2} \mathbb{E}[\text{vec}(\theta - m)' \nabla_\theta^2 G_\tau(m) \text{vec}(\theta - m)] \\ &= G_\tau(m) + \frac{1}{2} \text{tr}(\nabla_\theta^2 G_\tau(m) \Sigma_\theta),\end{aligned}$$

where the second step uses the trace identity $\mathbb{E}[v'Av] = \text{tr}(A \mathbb{E}[vv'])$ together with $\mathbb{E}[\text{vec}(\theta - m) \text{vec}(\theta - m)'] = \Sigma_\theta$. Rearranging yields

$$G_\tau(m) - \mathbb{E}_{\theta \mid \mathcal{D}_T}[G_\tau(\theta)] \approx -\frac{1}{2} \text{tr}(\nabla_\theta^2 G_\tau(m) \Sigma_\theta). \quad \blacksquare$$

Proof of the Variance Decomposition

Proof. The portfolio return is $r_{p,\tau+1}(\theta) = (w_b + \theta z_\tau)' R_{\tau+1}$. Treat θ as random with posterior mean m and covariance Σ_θ , independent of the future return $R_{\tau+1}$ conditional on the information set \mathcal{D}_T .² Apply the law of total variance with respect to the joint processes $(\theta, R_{\tau+1})$

$$\text{Var}(r_{p,\tau+1}) = \mathbb{E}_\theta[\text{Var}_R(r_{p,\tau+1} \mid \theta)] + \text{Var}_\theta(\mathbb{E}_R[r_{p,\tau+1} \mid \theta]).$$

The first term is

$$\begin{aligned}\mathbb{E}_\theta[\text{Var}_R(r_{p,\tau+1} \mid \theta)] &= \mathbb{E}_\theta[\text{Var}_R((w_b + \theta z_\tau)' R_{\tau+1})] \\ &= \mathbb{E}_\theta[(w_b + \theta z_\tau)' \Omega (w_b + \theta z_\tau)],\end{aligned}$$

where $\Omega = \text{Var}(R_{\tau+1})$. This is the market-risk term in Equation (8).

²This conditional independence holds because $R_{\tau+1}$ is a future realisation not contained in the estimation sample \mathcal{D}_T .

For the second term (estimation risk), write

$$\mathbb{E}_R[r_{p,\tau+1} | \theta] = (w_b + \theta z_\tau)' \mu_{\tau+1}, \quad \mu_{\tau+1} = \mathbb{E}[R_{\tau+1}].$$

This is linear in θ , so

$$\begin{aligned} \text{Var}_\theta(\mathbb{E}_R[r_{p,\tau+1} | \theta]) &= \text{Var}_\theta(z_\tau' \theta' \mu_{\tau+1}) \\ &= \mu_{\tau+1}' \text{Var}(\theta z_\tau) \mu_{\tau+1} \\ &= \mu_{\tau+1}' (z_\tau' \Sigma_\theta z_\tau) I_K \mu_{\tau+1} \\ &= z_\tau' \Sigma_\theta z_\tau \cdot \|\mu_{\tau+1}\|^2. \end{aligned}$$

The third equality uses the separable covariance structure assumed throughout i.e. $\text{Var}(\theta z_\tau) = (z_\tau' \Sigma_\theta z_\tau) I_K$. This yields the exact estimation-risk term used in Equation (8)

$$\text{Var}_\theta(\mathbb{E}_R[r_{p,\tau+1} | \theta]) = z_\tau' \Sigma_\theta z_\tau \cdot \|\mu_{\tau+1}\|^2.$$

Combining both terms

$$\text{Var}(r_{p,\tau+1}) = \mathbb{E}_\theta[\text{Var}_R(r_{p,\tau+1} | \theta)] + z_\tau' \Sigma_\theta z_\tau \cdot \|\mu_{\tau+1}\|^2.$$

The first term is market risk integrated over policy uncertainty. The second term is additional variance induced by uncertainty in θ , proportional to the quadratic form $z_\tau' \Sigma_\theta z_\tau$. PPP sets $\Sigma_\theta = 0$ and therefore ignores this term entirely, systematically understating portfolio risk whenever $\Sigma_\theta \neq 0$. ■

B Estimation

We solve for $\hat{\theta}_t$ via maximum a posteriori (MAP) estimation

$$\hat{\theta}_t = \arg \max_{\theta} \left\{ \sum_{s=1}^T U(w_s(\theta)' R_{s+1}) - \frac{1}{2\nu} \|\theta - M_t\|_F^2 \right\}. \quad (13)$$

The penalty term in Equation (13) is the log-prior contribution. It shrinks $\hat{\theta}_t$ toward the prior mean M_t with strength $1/\nu$, providing regularisation that reduces estimation variance. The PPP benchmark is the limiting case $\nu \rightarrow \infty$, in which the prior is uninformative and estimation risk is ignored as discussed in Proposition 1.

The portfolio return at each in-sample date s is $r_{p,s} = w_s(\theta)' R_{s+1}$, where $w_s(\theta) = \Pi(w_b + \theta z_s)$ and $\Pi(\cdot)$ bounds each position to the feasible set \mathcal{W} . Because Π is piecewise linear and differentiable, we apply the straight-through estimator and pass gradients given by

$$\frac{\partial \mathcal{L}_t}{\partial \theta_{k,\ell}} = \sum_{s=1}^{T_t} (1 + r_{p,s})^{-\gamma} R_{s+1,k} z_{s,\ell} \mathbf{1}\{k \in \mathcal{A}_s\} - \frac{\theta_{k,\ell} - [M_t]_{k,\ell}}{\nu}, \quad (14)$$

where $\mathcal{A}_s \subseteq \{1, \dots, K\}$ denotes the set of assets at date s and $(1 + r_{p,s})^{-\gamma} = U'(r_{p,s})$ is the CRRA marginal utility. The full gradient matrix is supplied analytically to standard L-BFGS-B optimization routine, which handles box constraints via projected quasi-Newton steps.

Given $\hat{\theta}_t$, we form a diagonal Gaussian approximation to the posterior. The diagonal of the Hessian of the negative log-posterior at $\hat{\theta}_t$ is

$$[H_t]_{k,\ell} = \sum_{s=1}^{T_t} \gamma (1 + r_{p,s})^{-(\gamma+1)} R_{s+1,k}^2 z_{s,\ell}^2 \mathbf{1}\{k \in \mathcal{A}_s\} + \frac{1}{\nu}, \quad (15)$$

with posterior variance $v_{k,\ell} = [H_t]_{k,\ell}^{-1}$. We draw M perturbations and average the implied

portfolio weights as follows

$$w_\tau^{\text{BPPP}} = \frac{1}{M} \sum_{m=1}^M w_\tau \left(\hat{\theta}_t + \epsilon^{(m)} \right), \quad \epsilon^{(m)} \sim \mathcal{N}(0, \text{diag}(v_t)), \quad (16)$$

where v_t collects all $v_{k,\ell}$ into a matrix of the same shape as θ . The Laplace approximation requires one MAP optimisation per rebalancing date, followed by M inexpensive Gaussian draws and linear weight evaluations, keeping the exercise feasible in the high-dimensional setting. Full Bayesian inference via Markov-Chain Monte Carlo is computationally prohibitive when $K \times L$ parameters are updated monthly over a 50-year sample.

Next, weights are projected onto the feasible set \mathcal{W} after averaging. All strategies share identical constraints. Individual positions are capped at $\pm 60\%$ (long or short any single factor) and gross exposure is bounded at 200% of capital. These constraints are the same across PPP and BPPP, so any performance difference reflects estimation-risk correction alone, not differential access to leverage. Both strategies rebalance monthly when conducting the out-of-sample exercise.

The out-of-sample evaluation uses an expanding estimation window with an initial length of $T_0 = 120$ months. At each subsequent rebalancing date t , all available history up to month t is used for MAP estimation, with the previous period's $\hat{\theta}_{t-1}$ serving as a warm start for L-BFGS-B. The prior variance ν_t follows Equation (10), growing with the window length so that the prior becomes progressively less restrictive as evidence accumulates relative to the signal dimension L . The prior mean is set to $M_t = \hat{\theta}_{t-1}$ throughout (Section 3.1), so that regularisation penalises deviations from the previous period's policy rather than from zero. This dynamic prior mean implements Bayesian shrinkage toward the investor's recent policy experience, providing a natural form of continuity in portfolio construction without hard constraints on turnover.

B.1 Estimation with a Horseshoe Prior

Estimation alternates MAP updates over $(\theta, \sigma^2, \tau, \{\lambda_{\ell,k}\})$, using the same portfolio objective and constraint pipeline as PPP and BPPP. The regularised local variance of the horseshoe prior,

$$\tilde{\lambda}_{\ell,k}^2 = \frac{c^2 \lambda_{\ell,k}^2 \tau^2}{c^2 + \lambda_{\ell,k}^2 \tau^2},$$

alternates between harder shrinkage when the product $\lambda_{\ell,k}\tau$ is small and the slab when it is large. Conditional on the current scales, the θ -step minimises the negative log-posterior

$$\hat{\theta}_t = \arg \max_{\theta} \left\{ \bar{U}(\theta) - \frac{1}{2T} \sum_{k,\ell} \frac{(\theta_{k,\ell} - M_{k,\ell})^2}{\tilde{\lambda}_{\ell,k}^2} \right\}, \quad (17)$$

where $\bar{U}(\theta)$ is the sample mean CRRA utility and $M_{k,\ell}$ is the prior mean. This step is solved with analytic gradients. Next, three quantities are updated. The residual scale σ^2 is the mean squared residual of the policy-scaled linear predictor against realised returns. The Pironen–Vehtari target,

$$\tau_{\text{PV}} = \frac{p_0}{L - p_0} \frac{\sigma}{\sqrt{T}},$$

translates the prior belief that roughly p_0 of the L signals carry genuine predictive content into a global shrinkage level. The current τ is blended toward this target,

$$\tau \leftarrow \rho \tau_{\text{old}} + (1 - \rho) \tau_{\text{PV}},$$

and the local scales are updated as

$$\lambda_{\ell,k}^2 \leftarrow \frac{|\theta_{k,\ell} - M_{k,\ell}|}{\sigma \tau} + 1,$$

so signals with large deviations from the prior mean receive less shrinkage. All updates include minor numerical safeguards for stability. Convergence is declared when changes in θ , τ , and λ all fall below a tolerance.

Prediction follows the same Monte-Carlo averaging as BPPP. Each coefficient is perturbed by a draw from the diagonal Laplace posterior around the MAP,

$$\epsilon_{k,\ell}^{(m)} \sim \mathcal{N}(0, v_{k,\ell}), \quad v_{k,\ell} = \left(\frac{1}{K^2} \sum_s c_s r_{s,k}^2 z_{s,\ell}^2 + \frac{1}{\tilde{\lambda}_{\ell,k}^2} \right)^{-1},$$

where $c_s = -U''(1 + r_{p,s})$ is the CRRA curvature at the MAP portfolio return. Weights are then averaged as in Equation (16). The posterior shrinkage factor for each signal,

$$\kappa_{\ell,k} = \frac{1}{1 + \tilde{\lambda}_{\ell,k}^2 \|z_\ell\|^2 / \sigma^2},$$

measures how far the posterior is from the prior mean.

C Additional Tables and Figures

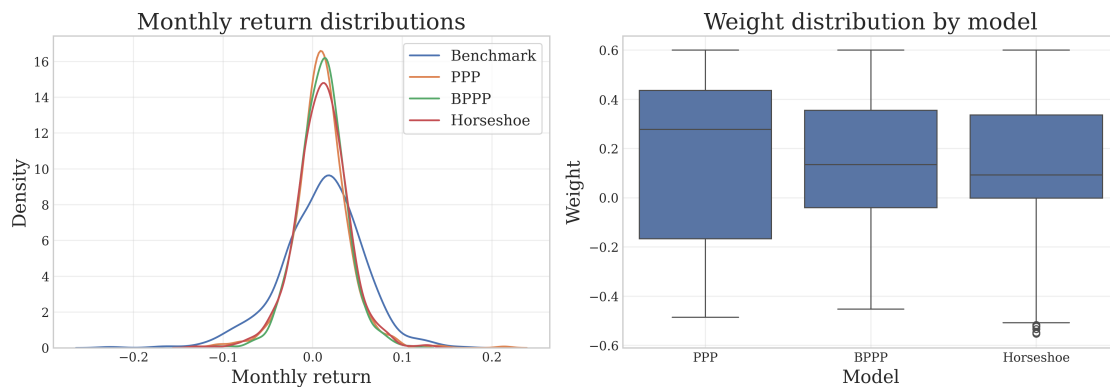


Figure A1: Return and Weight Distributions by Model

Notes: Left: kernel density estimates of monthly out-of-sample returns. Right: boxplots of factor weights across the out-of-sample period. BPPP produces a narrower weight distribution and a more symmetric, lighter-tailed return distribution than PPP, consistent with the overexposure correction of Proposition 1.

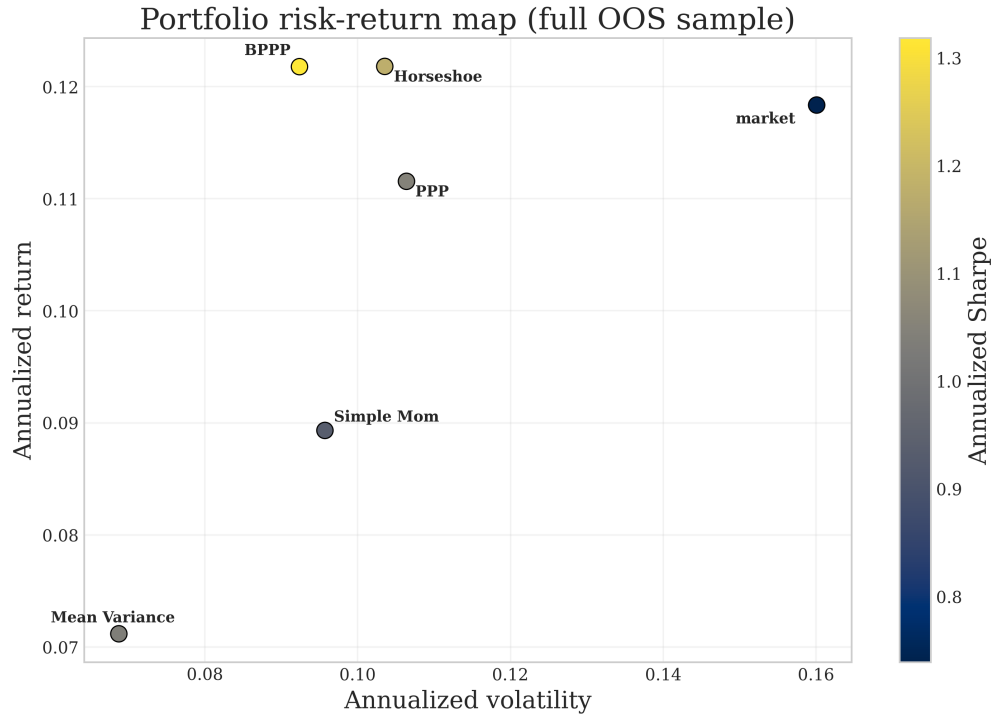


Figure A2: Portfolio Risk-Return Map (Full Out-of-Sample Period)

Notes: Annualised volatility–return space, 1973–2023. Colour encodes the Sharpe ratio.

Table A1: Economic Significance: Certainty Equivalents and Performance Fees

Portfolio	CE annual (%)	CE vs. Market (%)	Perf. Fee (bp)
BPPP	10.52	5.36	500
PPP	8.68	3.53	331
Horseshoe	9.90	4.74	443
Mean-Var	6.09	0.93	89
Benchmark	5.15	—	—

Notes: CE returns under exact CRRA utility, $\gamma = 5$. Performance fee: annual bp a benchmark investor would pay to switch to the given strategy.

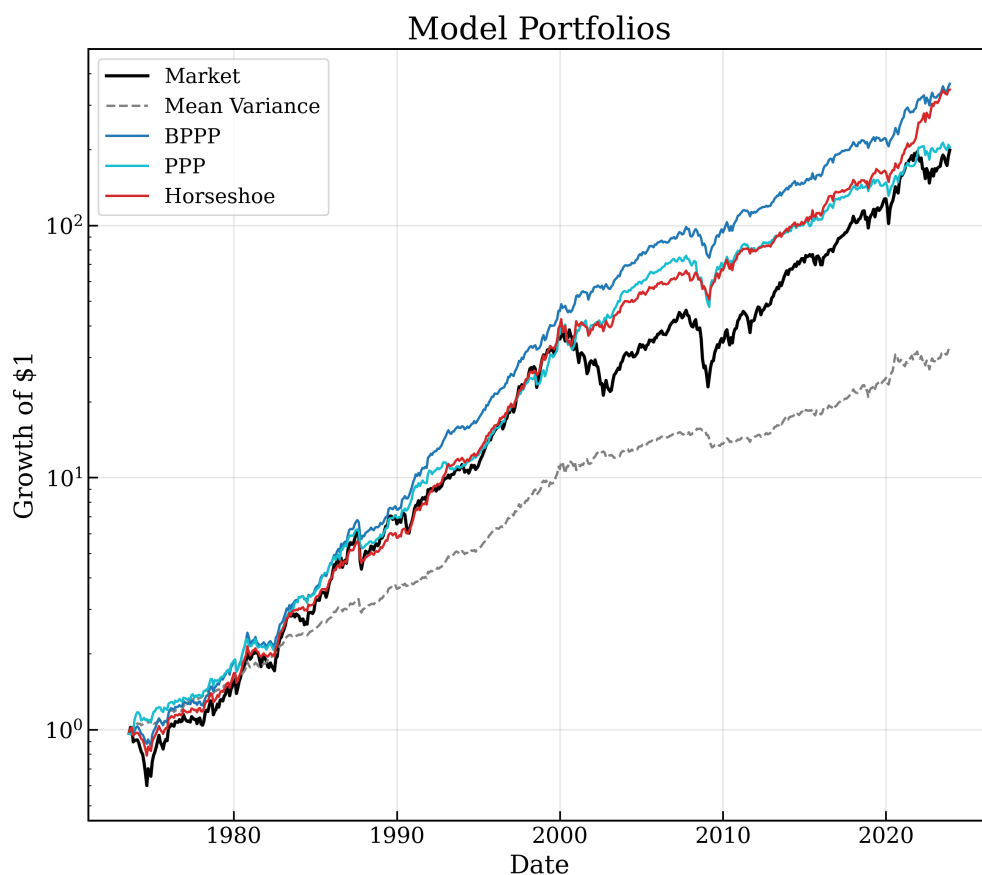


Figure A3: Cumulative Returns by Model

Notes: Cumulative portfolio wealth, expanding window, monthly rebalancing, initial training 120 months.

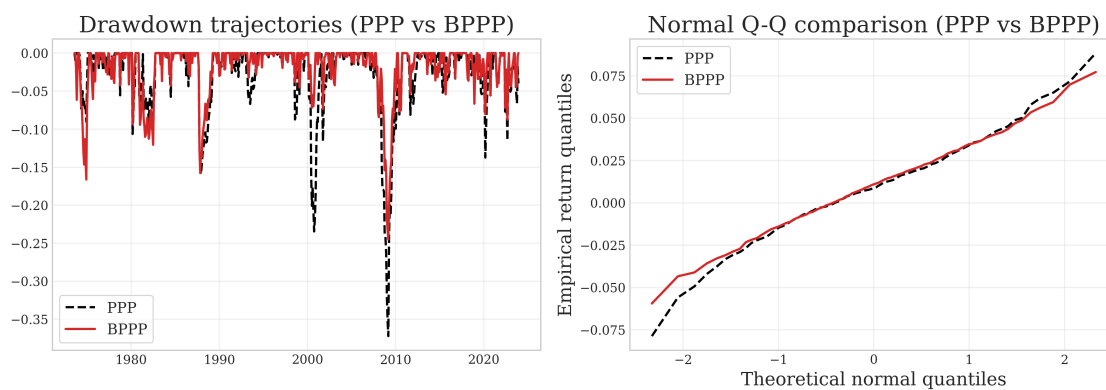


Figure A4: Drawdown and Normal Q-Q: PPP vs. BPPP

Notes: Left: drawdown from peak wealth. Right: normal Q-Q of monthly returns.

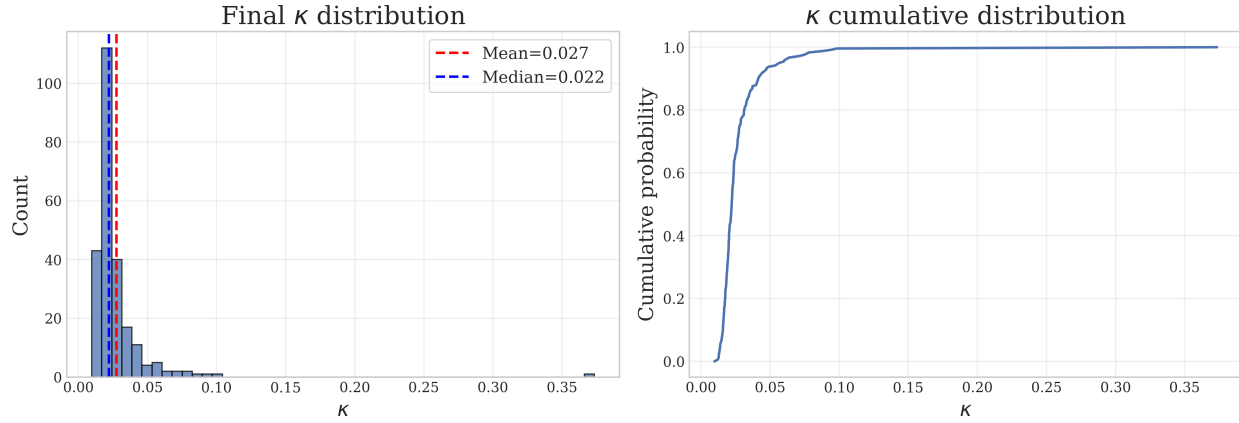


Figure A5: Distribution of Horseshoe Shrinkage Factors

Table A2: Prior Calibration Under Alternative Target Tilt Standard Deviations

δ	σ_θ	ν
0.20	0.0129	0.0005
0.35	0.0225	0.0015
0.50	0.0321	0.0031

Notes: $\sigma_\theta = \delta/\sqrt{L}$ and $\nu = \sigma_\theta^2 \cdot \max(T/L, 1)$ with $L = 242$. Baseline: $\delta = 0.35$.

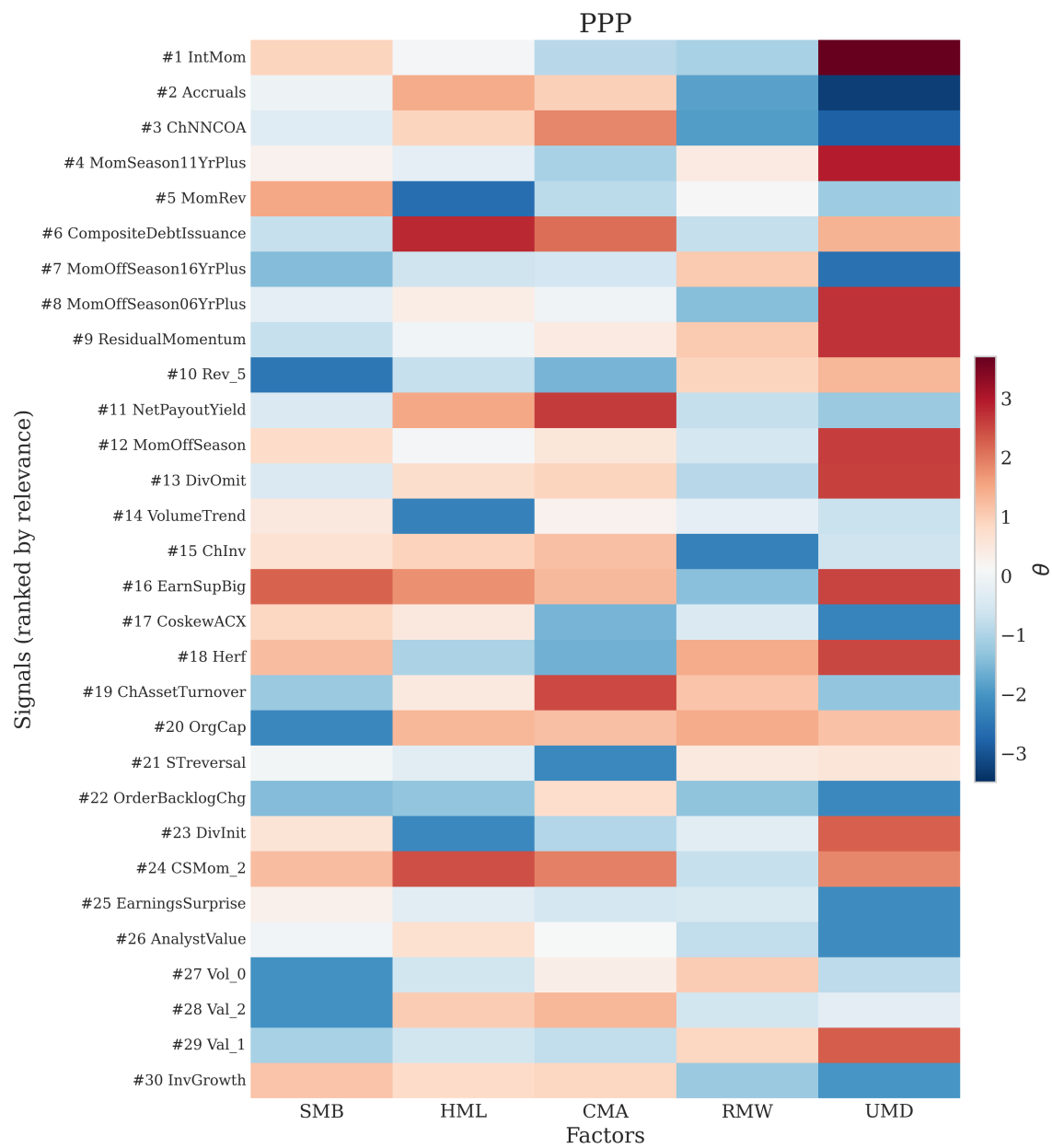


Figure A6: Top Signal Coefficients Across Models (I)

Notes: Heatmap of the largest signal interactions by absolute coefficient across PPP, BPPP, and Horseshoe.

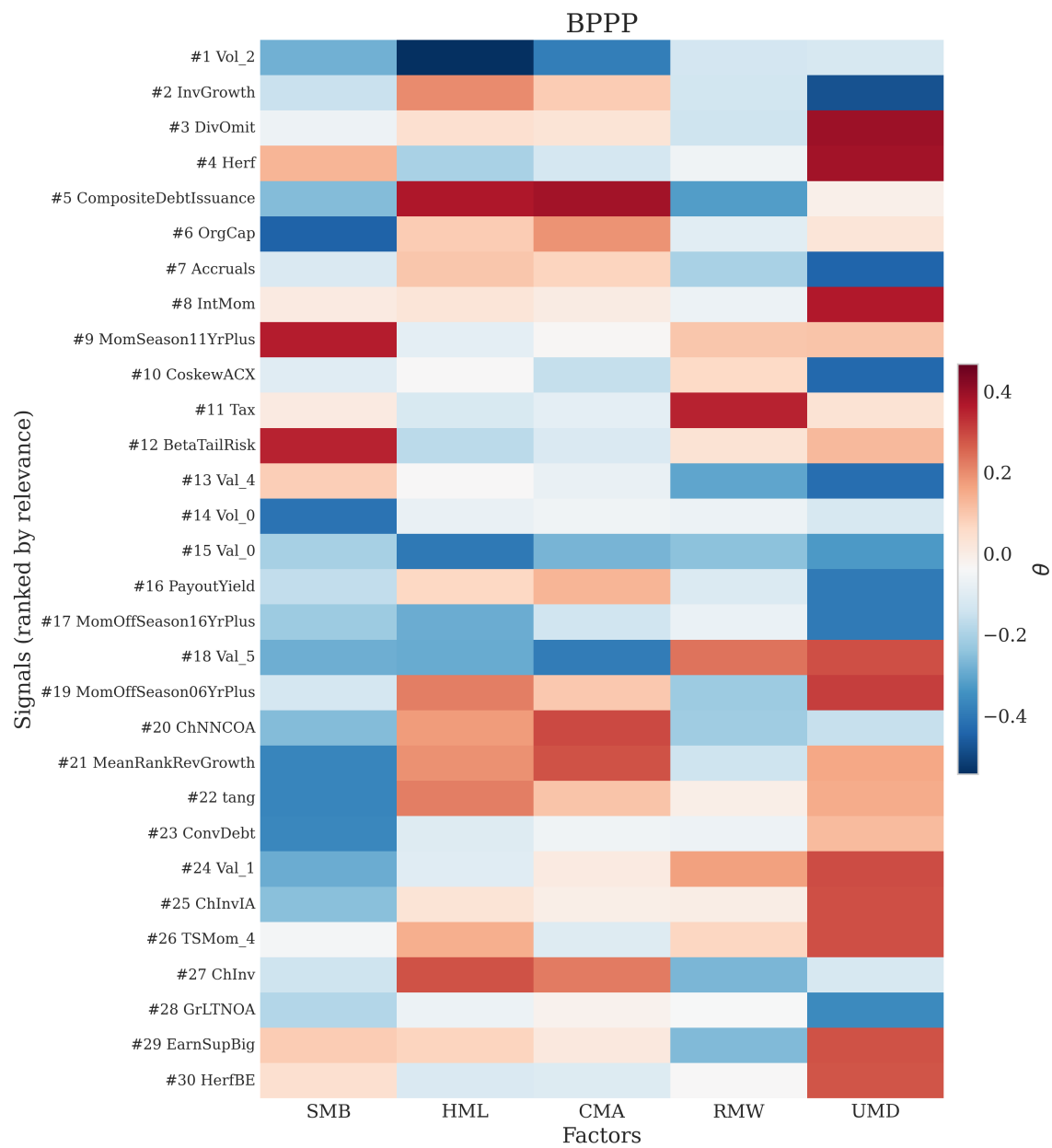


Figure A7: Top Signal Coefficients Across Models (II)

Notes: Heatmap of the largest signal coefficients by absolute coefficient across PPP, BPPP, and Horse-shoe.

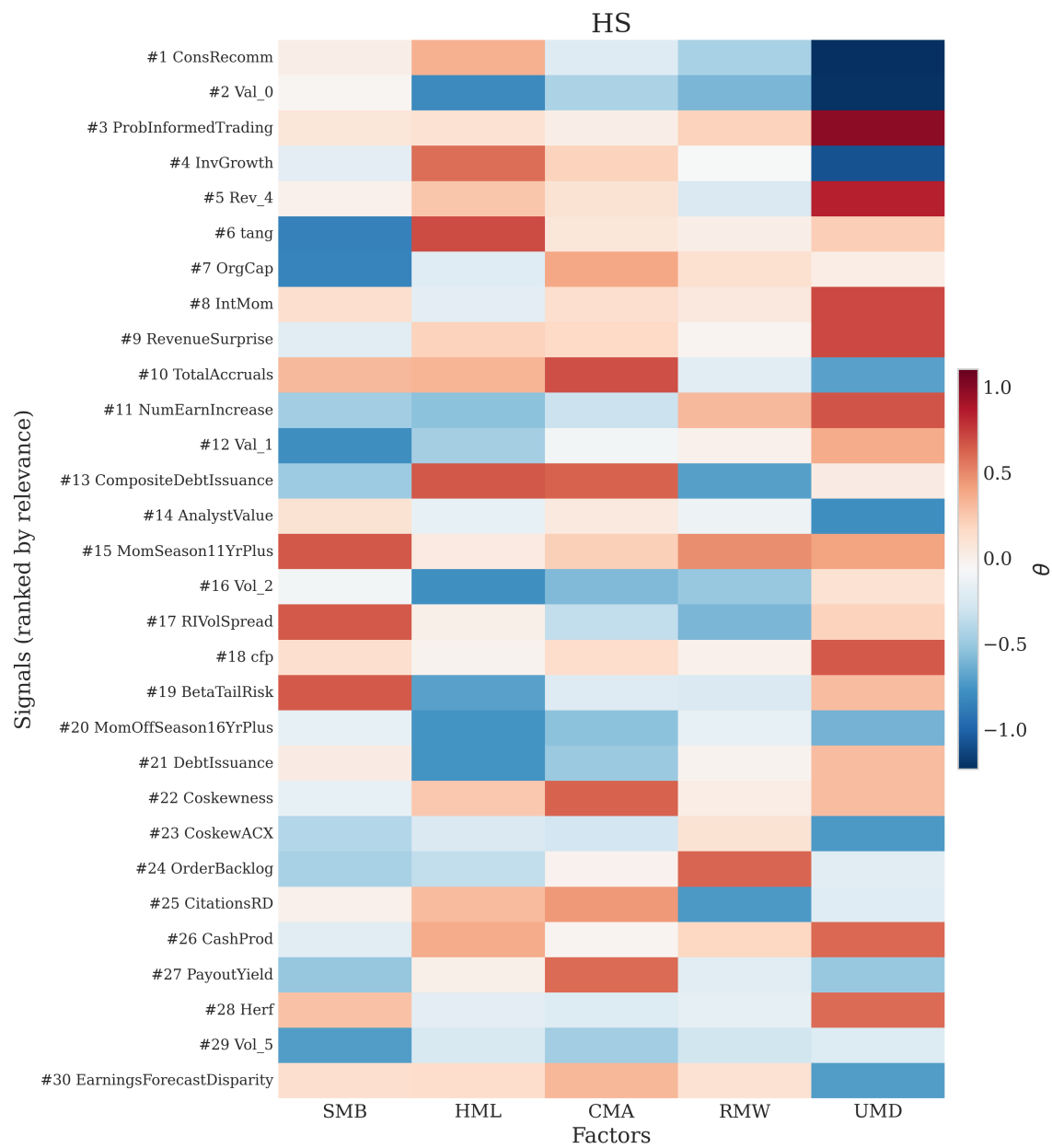


Figure A8: Top Signal Coefficients Across Models (III)

Notes: Heatmap of the largest signal coefficients by absolute coefficient across PPP, BPPP, and Horse-shoe.

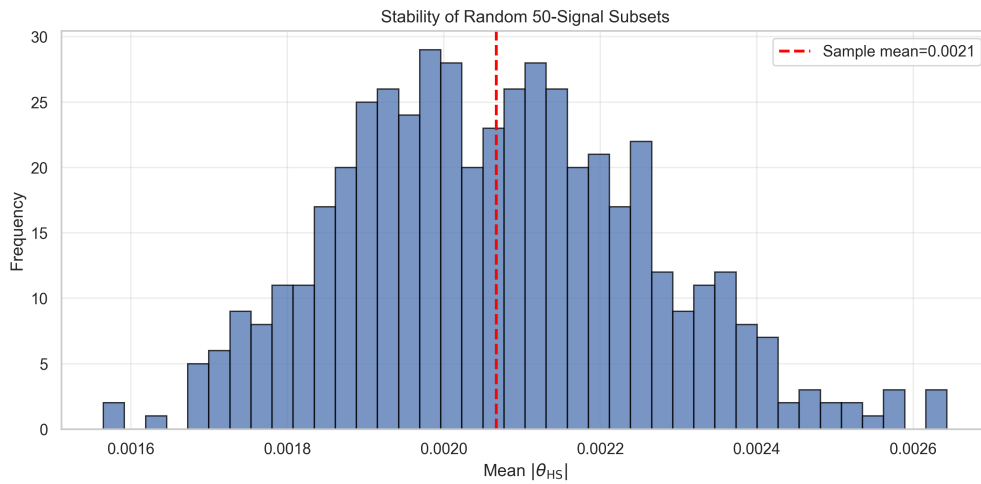


Figure A9: Signal Subset Stability: Bootstrap Distribution of Mean Horseshoe Coefficients

Notes: Distribution of mean absolute horseshoe coefficient across 500 draws of 50 signals from the full set of 242.

Table A3: Subset of Signals Referenced in the Paper

Signal	Description	Signal	Description
Accruals	Accruals	NumEarnIncrease	Earnings-increase streak length
AnalystValue	Analyst value	OrgCap	Organizational capital
BetaTailRisk	Tail-risk beta	PayoutYield	Payout yield
ChAssetTurnover	Change in asset turnover	ProbInformedTrading	Probability of informed trading
ChInv	Inventory growth	RIVolSpread	Realized-minus-implied volatility spread
ChNNCOA	Change in net noncurrent operating assets	ResidualMomentum	FF3-residual momentum
CompositeDebtIssuance	Composite debt issuance	RevenueSurprise	Revenue surprise
ConsRecomm	Consensus recommendation	Tax	Taxable income to income
CoskewACX	Daily-return coskewness	TotalAccruals	Total accruals
DivOmit	Dividend omission	VolumeTrend	Volume trend
EarnSupBig	Earnings surprise of large firms	cfp	Operating cash flow to price
Herf	Industry concentration (sales Herfindahl)	tang	Tangibility
IntMom	Intermediate momentum	Val.0	Valuation gap, Mkt
InvGrowth	Investment growth	Val.1	Valuation gap, SMB
MomOffSeason	Off-season long-horizon reversal	Val.4	Valuation gap, RMW
MomOffSeason06YrPlus	Off-season reversal, yrs 6–10	Val.5	Valuation gap, UMD
MomOffSeason16YrPlus	Off-season reversal, yrs 16–20	Rev.4	Reversal signal, RMW
MomRev	Momentum/reversal composite	Rev.5	Reversal signal, UMD
MomSeason11YrPlus	Return seasonality, yrs 11–15	Vol.0	Volatility-timing signal, Mkt
NetPayoutYield	Net payout yield	Vol.2	Volatility-timing signal, HML

Notes: The 40 signals listed are the subset of the total 242 signals used for estimation that are shown in the Tables and Figures throughout, those referenced in signal-level graphs (top-20 signal-factor interactions across PPP, BPPP, and Horseshoe). Data are monthly. Signals are standardized in expanding windows using only information available at each date. Estimation sample is 1963M7–2023M12; out-of-sample evaluation is 1973M8–2023M12 after a 120-month initial window. Signals not in the Val/Rev/Vol families are from [Chen and Zimmermann \(2022\)](#). Factor-timing signals (Val/Rev/Vol) follow [Haddad et al. \(2020\)](#) and are implemented as: for factor k , $Val_{k,t} = -\log\left(C_{k,t}/\exp\left[\frac{1}{60}\sum_{j=0}^{59}\log(C_{k,t-j})\right]\right)$, $Rev_{k,t} = -(r_{k,t-1} - \frac{1}{36}\sum_{j=0}^{35}r_{k,t-j})$, and $Vol_{k,t} = -\hat{\sigma}_{k,t}^{(12)}$ with $\hat{\sigma}_{k,t}^{(12)} = \sqrt{\frac{12}{11}\widehat{Var}_{12}(r_{k,\cdot})}$. Here $k \in \{0, 1, 2, 3, 4, 5\} = \{\text{Mkt}, \text{SMB}, \text{HML}, \text{CMA}, \text{RMW}, \text{UMD}\}$, and this table uses Val.0, Val.1, Val.4, Val.5; Rev.4, Rev.5; Vol.0, Vol.2. Acronyms follow those in the Open Source Asset Pricing Dataset.